analysis. Moreover, on the basis of the conclusions reached, it is necessary to discuss the Berson-Salem hypothesis in terms of electronic configurations rather than one-electron energies. The forbidden crossing of the ground state configurations in Figure 1, which is only facilitated in the triplet configuration, could be removed by placing one zwitterionic state (of 2_{op} or of 2_{cl}) below the biradical singlet.
(29) N. D. Epiotis, R. L. Yates, and F. Bernardi, *J. Am. Chem. Soc.*, **97**, 4198 (1975).
(30) The 3 × 3 CI procedure within the MINDO/2 approximation overestimates the importance of C-H hyperconjugation probably due to the neglect of overlap.[24] For the case presented here the conformation with $\beta = 90°$, $\gamma = 90°$ tends to be too low in energy compared to the conformation with $\beta = 0°$, $\gamma = 90°$. Because of this failure the rotational barrier of our procedure comes out too large. A reasoning will be given elsewhere.[24]
(31) R. Hoffmann, S. Swaminathan, B. G. Odell, and R. Gleiter, *J. Am. Chem. Soc.*, **92**, 7091 (1970).
(32) W. J. Hehre, L. Salem, and M. R. Willcott, *J. Am. Chem. Soc.*, **96**, 4328 (1974).

Characterization of the Anomalous Phosphorescence of *p*-Chlorobenzaldehyde in Polycrystalline Methylcyclohexane at 4.2 K[1a]

Omar S. Khalil and Lionel Goodman*

Contribution from the Wright and Rieman Chemistry Laboratories, Rutgers, The State University of New Jersey, New Brunswick, New Jersey 08903.
Received January 25, 1977

Abstract: Shpol'skii-type quasi-line phosphorescence spectra of *p*-chlorobenzaldehyde (PCB), and its deuterated derivatives, are studied in methylcyclohexane polycrystalline matrix at 4.2 K. The phosphorescence is composed of two subspectra at 44 cm^{-1} separation in PCB-h_5, a low-energy short-lived one ($\tau \sim 1$ ms) and a higher-energy long-lived one ($\tau \sim 12$ ms). Aldehyde group deuteration leads to the disappearance of the short-lived emission, while ring deuteration leads to changes in energies and relative quantum yields of the two emission systems. Thermal population of an upper state, aggregation, and different host crystalline modifications are excluded as origins of the multiple emissions. A two-site model is not directly ruled out experimentally but appears to require an abnormally large intermolecular contribution to the deuterium isotope effect on radiationless relaxation processes if the isotope effects on the spectra are to be explained. A two-state model involving an unrelaxed upper excited state is proposed. The salient features of this model are: large geometric dissimilarity between the two emitting states, and small efficiency for relaxation of the upper state through the lattice phonons. The main difficulty with this model is in the latter feature, requiring a weak host-guest interaction so that PCB in methylcyclohexane acts nearly like a relaxed free molecule. The deuteration effects are then explained by varying degrees of coupling between the two states as modulated by the isotope-dependent energy gap. Thermalization experiments and the details of the phosphorescence of PCB in MCH-d_{14} qualitatively support the model. Either the two site or the two-state model illustrate the inadequacy of current theories of radiationless transitions in molecules with closely spaced states in describing intermolecular contributions to electronic relaxation processes.

The effects of interstate coupling on photophysical properties of the lowest triplet states of aromatic aldehydes and ketones have attracted attention[1b-8] to the vibronic spectra[1b,6,7] and magnetic properties[2-5] involving such states. These and photochemical reactivity[8] are found to depend on $^3n\pi^*$-$^3\pi\pi^*$ interaction and hence in general terms on the energy separation $\Delta E(^3n\pi^*$-$^3\pi\pi^*)$.

An example of the sensitivity of triplet state properties to $^3n\pi^*$-$^3\pi\pi^*$ energy spacing is found in the simple aromatic aldehyde *p*-chlorobenzaldehyde (PCB). The phosphorescence vibrational structure[2] and magnetic properties[4] of this molecule show dependence on the energy gap. These properties can be explained by interstate mixing that increases inversely with the gap.

In this paper we report the phosphorescence spectra of *p*-chlorobenzaldehyde and its deuterated derivatives in methylcyclohexane (MCH) at 4.2 K. The purpose is to investigate the effect of a solid environment on radiationless processes in a molecule with closely spaced states.

In MCH, the lowest energy phosphorescences of PCB can be assigned as originating from a predominantly $^3n\pi^*$ state (vide infra). Very closely separated from this phosphorescence origin, at 44 cm^{-1} to higher energy, another phosphorescence origin is observed with attendant vibronic structure and lifetime indicating considerable interstate mixing between the $^3n\pi^*$ state and a closely spaced $^3\pi\pi^*$ level. The phosphorescence pattern is very sensitive to intramolecular deuteration. The short-lived $^3n\pi^*$-like emission disappears upon aldehyde group deuteration and is regained upon ring deuteration.

We examine the spectra of selectively deuterated *p*-chlorobenzaldehydes, e.g., PCB-d_1 (aldehyde hydrogen deuterated), PCB-d_4 (ring hydrogens deuterated) and PCB-d_5 (perdeuterated), to elucidate the origin of the deuterium isotope dependent multiple phosphorescence. We establish that the two phosphorescence spectra do not originate from thermal population of upper states, aggregation, different PCB ground state conformations, or different crystalline phases in the matrix. Thus a two site or a single-site two-state model interprets the multiple phosphorescence. However, neither is found satisfactory in terms of present theories of radiationless transition.

Experimental Section

PCB (Matheson Coleman and Bell) was vacuum sublimed twice and then zone refined (50 passes, 3 cuts, repeated twice). Deuterated derivatives were synthesized[9-11] by Dr. Ronald Ruden and were purified by multiple recrystallizations from *n*-hexane followed by vacuum sublimation. A gift of PCB-d_1 was also received from Professor D. S. Tinti, of the University of California at Davis, and was found to give identical results.[12] NMR, Raman, and mass spectral analyses of PCB-d_1 revealed isotopic purity greater than 99.5%. NMR analyses of PCB-d_4 reveals 2.5% PCB-d_3 distributed approximately equally between the two mono ring hydrogen isotopes. There are no detectable

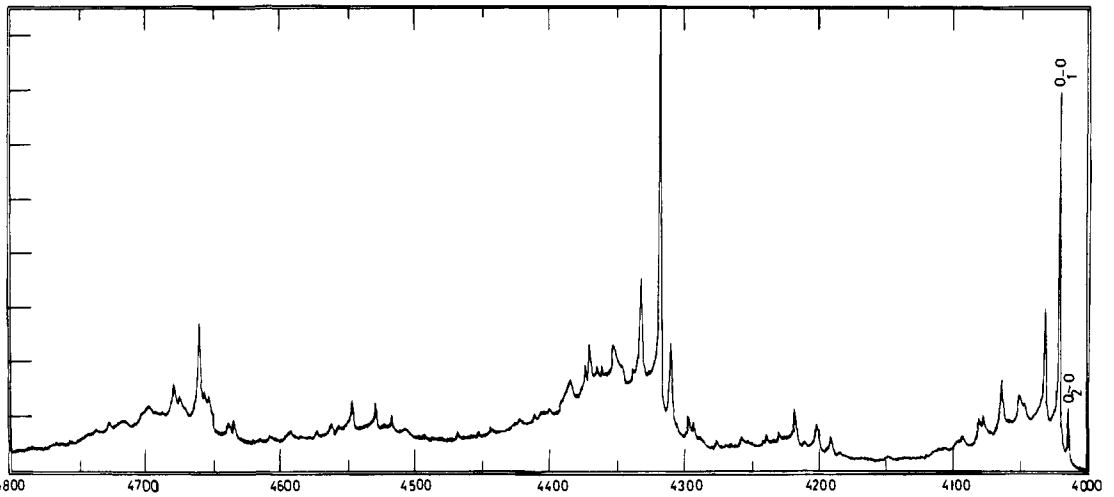

Figure 1. Phosphorescence spectrum of PCB in MCH at 4.2 K. Lamp excitation. O_1 refers to the origin of the short-lived phosphorescence and O_2 to the origin of the long-lived phosphorescence.

amounts of other possible isotopic impurities. PCB-d_5 was prepared by repeating the preparative procedure[9] on PCB-d_4. The isotopic purity in this case was in the vicinity of 95%.

Spectra in MCH were recorded for slowly cooled samples, in the vapor above liquid nitrogen. Sharp Shpol'skii-type spectra were only obtainable for such slowly cooled samples. Rapid cooling gave broad spectra. The intensity distribution of the various bands in the spectra was independent of the concentrations in the range 1×10^{-5}-2×10^{-2} M. A broad background emission was observed above 5×10^{-3} M, probably due to molecular aggregates. All samples were degassed by freeze-pump-thaw cycles and were sealed in thin Pyrex tubes.

The phosphorescence spectra were recorded by a previously described experimental set-up.[13,14] Excitation bandwidth was 8000 cm^{-1} centered around 3200 Å, extending into both $S_1(n\pi^*) \leftarrow S_0$ and $S_2(L_b) \leftarrow S_0$ regions. Identical results were obtained by narrow line excitation at 3000 and at 3200 Å from a chromatix CMX-4 flash lamp excited frequency doubled tunable dye laser or the 3371-Å line from a pulsed nitrogen laser.

Excitation spectra were recorded with an EMI 6256S photomultiplier using a 500 W high-pressure xenon lamp and a Spex ¾ M monochromator for excitation and monitoring the change in the total phosphorescence intensity passed by a 0.3 cm Corning CS 3-72 cut-off filter.

Phosphorescence decay curves were obtained using a variable speed phosphoroscope, with the spectrometer set at the O-O region of the phosphorescence at a slit width of 200 μm. The signal from the photomultiplier tube was fed into a Tektronix 502A oscilloscope and photographed. The decay curves for the two components were obtained photographically from oscilloscope traces using a variable speed phosphoroscope. The reported lifetime is the average of five separate decays.

Intensity variation of the two phosphorescence origins as the sample temperature increased was qualitatively studied by repeatingly scanning the origin region as the liquid helium evaporated. The ratio of the intensities of each origin to its intensity at 4.2 K could thus be determined. Alternatively the spectrometer was set at each origin wavelength and the intensity monitored as a function of time. Attempts to study variation of lifetimes with increasing temperature were unsuccessful because of the small lifetime/temperature resolution in our experiment.

Results

(I) PCB Phosphorescence in Methylcyclohexane Matrix. (A) General Features. The Shpol'skii-type quasi-linear phosphorescence spectrum of PCB-h_5 in slowly cooled polycrystalline MCH matrix at 4.2 K is shown in Figure 1. The spectrum was taken without the interposition of a phosphoroscope. The origin region (Figure 2a) has a moderately strong sharp band (half-bandwidth 5 cm^{-1}, the instrument limited experimental resolution) at 24 937 cm^{-1}, followed by a stronger sharp band at 24 893 cm^{-1}, a sharp band at 24 832 cm^{-1}, and weaker

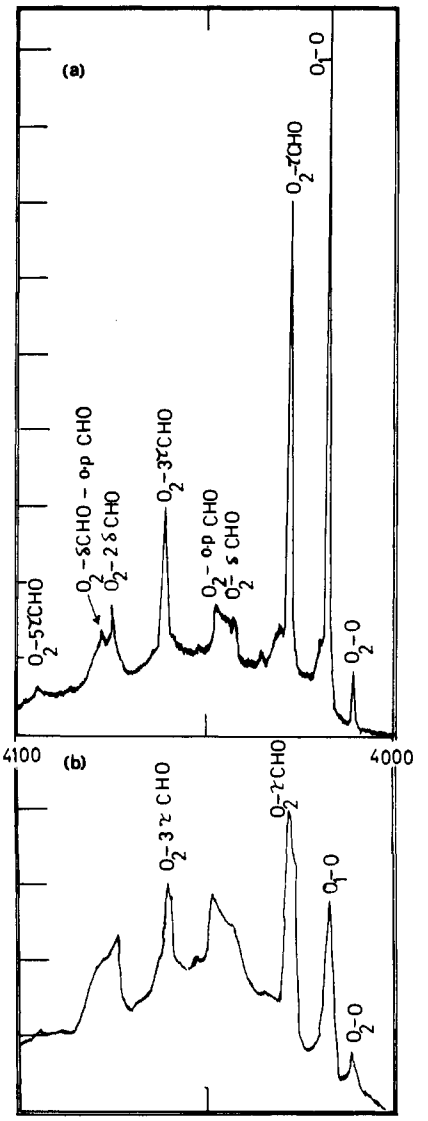

Figure 2. The O-O region of the phosphorescence spectrum of PCB in MCH at 4.2 K. See text and Table I for alternative assignments. τCHO refers to the CHO torsional mode, δCHO and o.p.CHO refer to the in-plane and out-of-plane CHO bending modes, respectively: (a) no phosphoroscope, N_2 laser excitation; (b) with phosphoroscope, lamp excitation. See text and Table I for alternative assignments.

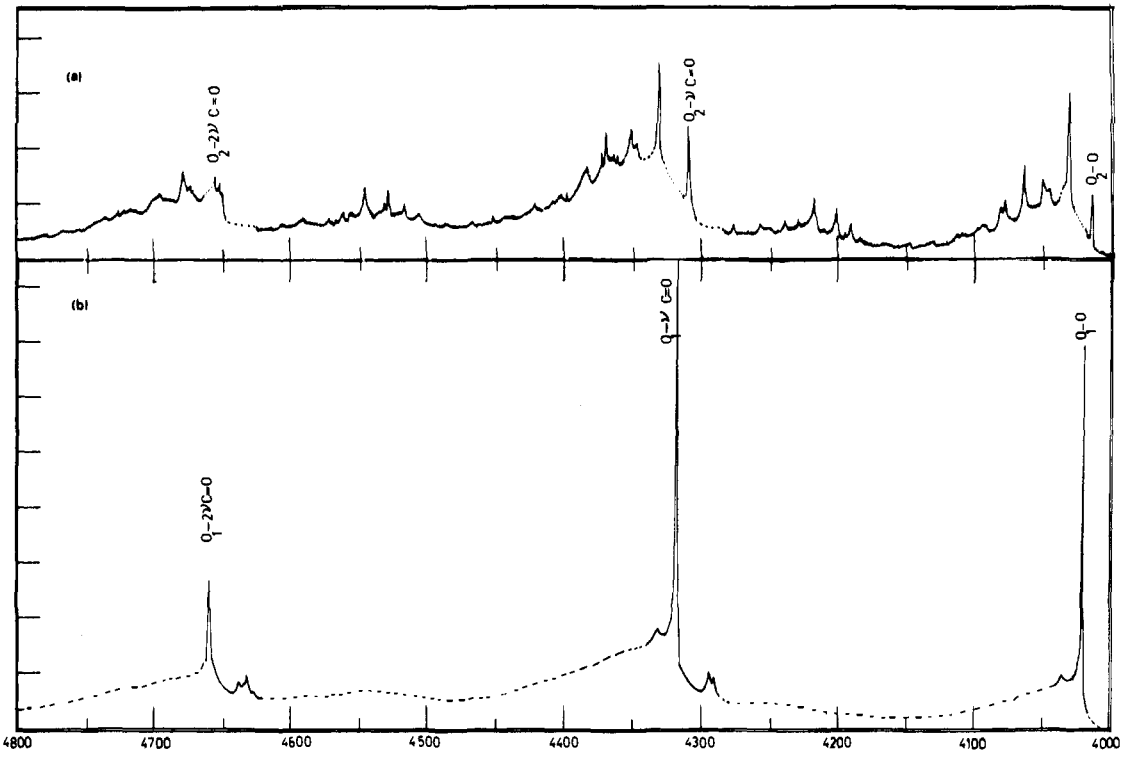

Figure 3. Synthesized phosphorescence spectra of PCB in MCH at 4.2 K. ν(C=O) refers to the carbonyl stretching mode: (a) long-lived phosphorescence; (b) short-lived phosphorescence.

Table I. Vibrational Analysis of the Origin Region of the Phosphorescence Spectrum of *p*-Chlorobenzaldehyde in Methylcyclohexane at 4.2 K

$\bar{\nu}$,[a,c] cm^{-1}	$\Delta\bar{\nu}$, cm^{-1}	Rel[d] intensity	Assignment[b]
24 937	0	100	O_2-O
24 893	44	684	O_1-O
24 832	105	318	O_2-τCHO
24 746	191	32	O_2-δCHO
24 712	225	58	O_2-ωCHO
24 630	307	105	O_2-3 × τCHO or O_2-τCHO-δCHO
24 557	380	63	O_2-2 × δCHO
24 533	404	21	O_2-δCHO-ωCHO
(24 447)	(490)	10	O_2-combination

[a] Corrected to vacuum. [b] Mode designations are: τCHO, aldehyde torsion, δCHO, aldehyde in-plane bend, ωCHO, aldehyde out-of-plane wag. [c] From either O_1 or O_2 origins as noted under assignment column. Parentheses refer to uncertain wavenumber due to band broadness. [d] Not corrected for phototube response.

broader bands at 24 746, 24 630, and down to 24 330 cm^{-1}. Some weak bands appear in the region 300–1300 cm^{-1} to the red of the origin. The vibrational pattern in the origin region is repeated four times at ~1715 cm^{-1} intervals, which corresponds to the ν(C=O) symmetric stretching frequency.

The phosphorescence in MCH decays nonexponentially, suggesting two component lifetimes. It was possible to resolve two decays 0.9 ± 0.1 and 12 ± 3 ms. The time-resolved experiments reveal that the 24 893 cm^{-1} band and the 1715 cm^{-1} progression built on it have the short lifetime and those vibronic bands built on the 24 937 cm^{-1} band have the long lifetime. Thus the phosphorescence spectrum contains two different subspectra. This is demonstrated for the O-O band region in Figures 2a and 2b, where the unchopped phosphorescence using N_2 laser excitation and the slowly chopped phosphorescence using lamp excitation are respectively displayed. The apparent loss of resolution between Figures 2a and 2b is due

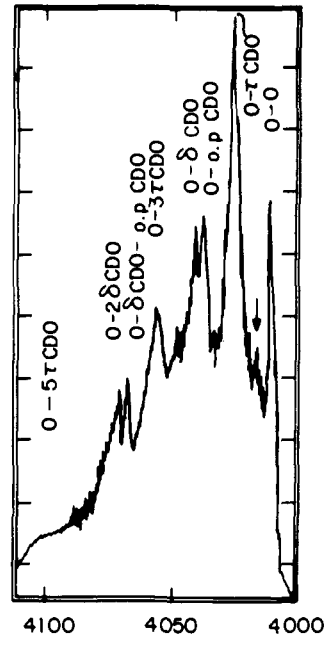

Figure 4. The O-O region of the phosphorescence spectrum of PCB-d_1 in MCH at 4.2 K. Lamp excitation. Arrows point to PCB-h_5 isotopic impurity bands. The vibrations shown for the O-O region are repeatedly built on *n* quanta of ν(C=O). See text and Table II however for alternative assignments.

to the wider slits necessitated by intensity attenuation caused by the chopper. We designate the 24 937 cm^{-1} and the 24 893 cm^{-1} bands as O_2 and O_1 respectively and consider them as the origins of the two subspectra.

(B) Subspectrum II. The long-lived subspectrum, built on the 24 937-cm^{-1} origin (O_2), is synthesized in Figure 3a by subtracting from the full spectrum those bands attenuated by progressively slower chopper seeds. In the origin region (Figure 2), except for the O_1 origin at 24 893 cm^{-1}, all resolved bands belong to subspectrum II. Band listings and assignments in the

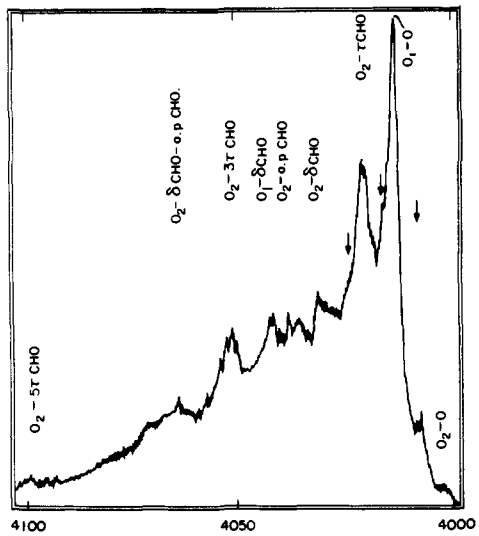

Figure 5. The O-O region of the phosphorescence spectrum of PBC-d_4 in MCH at 4.2 K. Lamp excitation. Arrows point to PCB-d_3 impurity bands. The vibrations shown for the O-O region are repeatedly built on n quanta of ν(C=O). See text and Table III for alternative assignments.

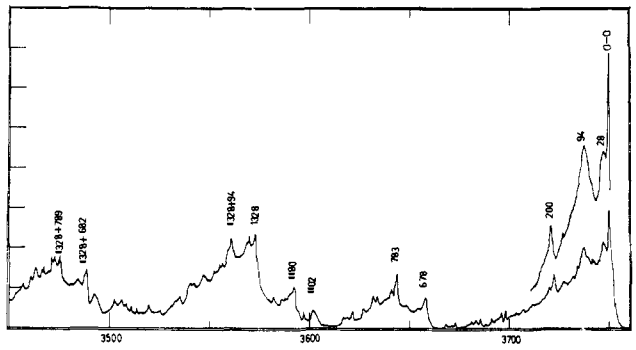

Figure 6. Phosphorescence excitation spectrum of PCB-h_5 in MCH in the $S_1 \leftarrow S_0$ region at 4.2 K. The upper spectrum is the origin region under high gain conditions.

origin region are given in Table I and are discussed in subsequent sections.

(C) Subspectrum I. The short-lived subspectrum is synthesized in Figure 3b by a similar procedure to the one used in synthesizing Figure 3a. The spectrum is simple exhibiting a single intense band in the region 0-2000 cm^{-1} to the red of the 24 893 cm^{-1} at 23 179 cm^{-1}, i.e., separated from O_1 by 1714 cm^{-1}. It can be definitely assigned to the ν(C=O) symmetric stretching vibration. The same interval is observed in a progression of three bands (Figure 3b). The only other bands are weak.

(D) PCB-d_1 Phosphorescence. The origin region of PCB-d_1 phosphorescence in MCH at 4.2 K is shown in Figure 4. The phosphorescence decays exponentially with a lifetime of 10-12 ms. The phosphorescence origin lies at 24 943 cm^{-1}, i.e., displaced 6 cm^{-1} from O_2 in PCB-h_5. A series of very weak bands with frequencies exactly matching those of PCB-h_5 phosphorescence also appear. Their intensity is accounted for by no greater than 1% isotopic impurity.

The striking feature of the phosphorescence from PCB-d_1 is that subspectrum I is absent.

(E) PCB-d_4 Phosphorescence. The origin region of the phosphorescence is shown in Figure 5. *As in PCB-h_5 two subspectra are found resembling those in PCB-h_5.* The relative intensity, however, of subspectrum II compared to that of subspectrum I is substantially reduced, probably by a factor of 3 from that in PCB-h_5.

Table II. Vibrational Analysis of the O-O Band Region of the Phosphorescence Spectrum of p-Chlorobenzaldehyde-d_1 in Methylcyclohexane at 4.2 K

$\bar{\nu}$,[a,c] cm^{-1}	$\Delta\bar{\nu}$,[c] cm^{-1}	Rel intensity[d]	Assignment[b]
24 943	0	100	O-O
24 937	6	4	O_2-O PCB-h_5 isotopic impurity
24 845	98	250	O-τCDO
24 776	167	70	O-ωCDO
24 751	192	60	O-δCDO
24 648	295	40	O-3 × τCDO or O_2-τCDO-δCDO
24 581	362	25	O-ωCDO-δCDO
24 562	381	20	O-2 × δCDO
(24 479)	(464)	10	O-5τCDO (?)

[a-d] See Table I footnotes.

The two subspectra are separated by 65 cm^{-1}. The O_2-O origin lying at 24 980 cm^{-1}. Subspectrum I is built on a sharp origin at 24 918 cm^{-1}. Both subspectra exhibit a 1712-cm^{-1} progression of 3-4 ν(C=O) stretching modes.

(F) PCB-d_5 Phosphorescence. The phosphorescence of PCB-d_5 in MCH was complicated by isotopic impurities which made vibrational assignments difficult. However, *the two-subspectra pattern observed in PCB-h_5 could be recognized.*

(II) $S_1 \leftarrow S_0$ Phosphorescence Excitation Spectrum of PCB in MCH. The $S_1 \leftarrow S_0$ phosphorescence excitation spectrum of PCB-h_5 in MCH at 4.2 K is shown in Figure 6 and is discussed in a later section.

Discussion

(I) Vibrational Analysis of the Origin Region. In order to assign the long-lived subspectrum of PCB-h_5, we turn to the origin band region of PCB-d_1 phosphorescence shown in Figure 4. Because of the unique long-lived phosphorescence, vibrational assignments are simpler than for the two-component PCB-h_5 spectrum.

Four bands appear in the region 0-200 cm^{-1} to lower wavenumber from the origin. These are at 6, 98, 167, and 192 cm^{-1} (Table II). The highest energy one is the O_2-O band of PCB-h_5 isotopic impurity. The strong band at 98 cm^{-1} can only be assigned to the torsional CDO vibration. The 167-cm^{-1} band corresponds to a Raman band at 159 cm^{-1} and can be assigned to the CHO out-of-plane wagging vibration ω(CHO).[15,16] The band at 192 cm^{-1} does not match any Raman frequency. Despite this discrepency the shifts on going to PCB-h_5, PCB-d_4, and PCB-d_5 seem to establish this as a vibronic band rather than an independent origin, i.e., from a site. This band then probably arises from the PhCHO in-plane bending mode δ(CHO).

Returning to PCB-h_5 the two bands appearing at 100-200 cm^{-1} to lower wavenumber from O_2 with approximately the same lifetime are at 105 and 191 cm^{-1} (Table I). The assignments are parallel to those made for PCB-d_1 i.e., 105 cm^{-1}, τ(CHO), 191 cm^{-1}, δ(CHO), respectively. The weak 225-cm^{-1} band, which does not match any infrared or Raman frequency, is tentatively assigned as a medium shifted ω(CHO). However, the possibility of a site band is not completely ruled out.

Of the three bands attributed to the CHO group, the torsional mode is the most intense, exceeding the intensity of the O_2-O band by at least a factor of 3 (Table II).

The relatively sharp peak at 24 630 cm^{-1}, corresponds to O_2-307 cm^{-1}, a frequency interval which can be assigned to any one of the following: the C-Cl out-of-plane bending vibration observed at 310 cm^{-1} in the Raman spectrum of PCB, the O_2-3 × τ(CHO) frequency expected at 325 cm^{-1}, or the O_2-τ(CHO)-δ(CHO). However, it shifts to 295 cm^{-1} in

Table III. Vibrational Analysis of the O-O Band Region of the Phosphorescence Spectrum of *p*-Chlorobenzaldehyde-d_4 in Methylcyclohexane at 4.2 K

$\bar{\nu}$,[a,c] cm^{-1}	$\Delta\bar{\nu}$, cm^{-1}	Rel intensity[d]	Assignment[b]
24 980	0	100	O_2-O
24 952	28	250	Site: O_1-O or O-O d_3 impurity
24 915	65	5000	O_1-O
24 874	106	1150	O_2-τCHO
24 807	173	500	O_2-δCHO
24 763	217	300	O_2-ωCHO
24 736	244	500	O_1-δCHO
24 678	302	520	O_2-3 × τCHO or O_2-τCHO-δCHO
(24 593)	(387)	300	O_2-δCHO-ωCHO

[a-d] Footnotes as in Table I.

PCB-d_1 and 302 cm^{-1} in PCB-d_4, eliminating the C-Cl mode and suggesting a combination of aldehyde group fundamentals.

Two moderately intense bands appear at 380 and 404 cm^{-1} from O_2. The 404-cm^{-1} band is the weaker one. In PCB-d_1 these bands have shifted to 362 and 381 cm^{-1} from the origin. The large aldehyde deuteration shift of the 404-cm^{-1} band allows assignment to combination of the aldehyde-deuteration sensitive CHO out-of-plane wagging mode and some other mode. The probable interpretation is ω(CHO) + δ(CHO) based on the close frequency agreement (Tables I and II) and the shift to 362 cm^{-1} in PCB-d_1. The 380-cm^{-1} band could result from two quanta of the aldehyde-deuteration insensitive CHO in-plane bending vibration.

The weak band in the vicinity of O_2-500 cm^{-1} shifts to 464 cm^{-1} in PCB-d_1, establishing that it represents a combination band in CHO modes.

(II) Origin of Multiple Phosphorescences. Multiple phosphorescences, while rare in low-temperature environments, have usually been accounted for by system artifacts, e.g., different solvent phases, aggregation, sites, etc. The anomaly at hand is the observed deuterium isotope dependent multiple phosphorescence (i.e., subspectra I and II appear in PCB-h_5 and -d_4, but only subspectrum II in PCB-d_1).

The first two bands in the phosphorescence spectrum of PCB in MCH were tentatively interpreted[1b] as split O$^{\pm}$ origins due to a double minimum potential surface for the $^3n\pi^*$ state for displacement along the CHO torsional coordinate. In this case the $^3n\pi^*[O^+] \rightarrow S_0$ transition is allowed and hence would appear like the normal $^3n\pi^* \rightarrow S_0$ spectrum; the $^3n\pi^*[O^-] \rightarrow S_0$ is forbidden and hence vibrationally allowed for out-of-plane modes. The newly acquired intramolecular deuterium isotope data are inconsistent with this interpretation. Since ring deuteration should have little or no effect on the O$^{\pm}$ separation, the increase in separation of the short and long-lived origins from 44 cm^{-1} in PCH-h_5 to 65 cm^{-1} in PCB-d_4 disfavors this model.

We now examine possible sources of the two observed phosphorescence subspectra of PCB-h_5 in MCH.

(1) Thermal Population of an Upper State. Thermal population of an upper $^3\pi\pi^*$ has been suggested for PCB in aromatic matrices at temperatures >77 K.[2] However, the short lifetime of the lower $^3n\pi^*$-like state and the small Boltzmann factor for two states separated by 44 cm^{-1} at 4.2 K eliminates any possibility of population of the upper state.

(2) Superposition of Monomeric Molecules and Molecular Aggregates. A dual emission observed in acetophenone[17] has been proposed[18] to occur by this kind of a mechanism. But the invariance of the phosphorescence spectra to concentration changes in the range 1 × 10^{-5}-5 × 10^{-3} M is contrary to this possibility. Further, the broad spectra observed at higher concentration and upon rapid cooling suggest that molecular aggregates produce broad rather than sharp bands.

(3) Two Sites in Which Molecules Have Different Conformations in the Ground State. The two phosphorescences observed for xanthone in 3-methylpentane glass[21] are believed to be due to different ground state conformations[22] for example. If this is the case for PCB in MCH, the vibrationally rich long-lived phosphorescence system would correspond to a torsionally distorted molecule and the vibrationally simple short-lived phosphorescence to a planar, or nearly planar, one. The isotope effect on the spectra will be determined by the effect on equilibrium between the two conformers. Since the torsional frequency observed from the long-lived phosphorescence spectrum is 104 cm^{-1}, identical to the 105 cm^{-1} value observed in vapor-phase IR spectra[16] (referring presumably to an undistorted molecule), the curvatures are similar. Aldehyde group deuteration is, therefore, predicted to not importantly affect the conformer equilibrium. Any deuteration effects on the spectra should simply lead to nearly identical shifts in the two-band systems. The observed deuteration effects on PCB spectra are then difficult to rationalize by two different ground state conformations.

(4) Molecules Embedded in Two Different Crystalline Phases. Benzene exhibits two phosphorescence spectra in the two crystalline modifications of cyclohexane.[23] Analysis of matrix perdeuteration effects and cooling rates on the phosphorescence of PCB in MCH and perdeuterio-MCH indicates that the phosphorescence spectrum of PCB is highly sensitive to the guest-host interaction.[14] Two sets of spectra are observed in MCH-d_{14}, one similar to that observed in MCH-h_{14}, the other a $^3\pi\pi^* \rightarrow S_0$ phosphorescence similar to that observed in aromatic matrices.[24] These observations were interpreted as due to two crystalline modifications of MCH, the one with the smaller gas to crystal shift is stable in slowly cooled MCH-h_{14}, the other is stable in slowly cooled MCH-d_{14}.

The important point is that neither subspectrum I nor subspectrum II appear by itself for any cooling rate in either MCH-h_{14} or MCH-d_{14}. The implication is that the two subspectra pattern observed in slowly cooled MCH-h_{14} is characteristic of PCB molecules in one crystalline modification of MCH and is not interpretable as due to PCB in two crystalline modifications of the solid environment.

(5) Molecules occupying different sites, i.e., molecules having the same equilibrium geometry but occupying different microenvironments in their ground state. Ground state sites having different energies arising from minor differences in crystal fields lead to triplet state molecular ensembles with different potential surfaces and consequently possible different electronic assignments.

INDO calculations on benzaldehyde predict the $^3n\pi^*$ potential curve to have curvature higher than either that of the ground and $^3\pi\pi^*$ states for displacement along the CHO torsional coordinate.[22] This is because the n and π^* orbitals are respectively substantially antibonding and bonding in the C_{ring}-$C_{aldehyde}$ bond region. The lowest energy $^3\pi\pi^*$ potential curve is predicted to have the lowest curvature along this coordinate. Transferring these conclusions to PCB suggests that the $^3\pi\pi^*$ state should be the most susceptible state to potential surface distortion arising from either crystal or nonadiabatic vibrational-electronic perturbations. The predicted state ordering and schematic representation of curvatures for a free PCB molecule are illustrated in Figure 7A.

A two-site model is illustrated in Figure 7B. In this model, one of the two geometrically dissimilar lowest energy excited states in $^3\pi\pi^*$-like. Its minimum energy conformation is distorted along the CHO torsional coordinate, as well as the ν(C=O) symmetric stretching coordinate relative to the ground state equilibrium geometry. This is consistent with the strong activity of the τ(CHO) mode in subspectrum II. The

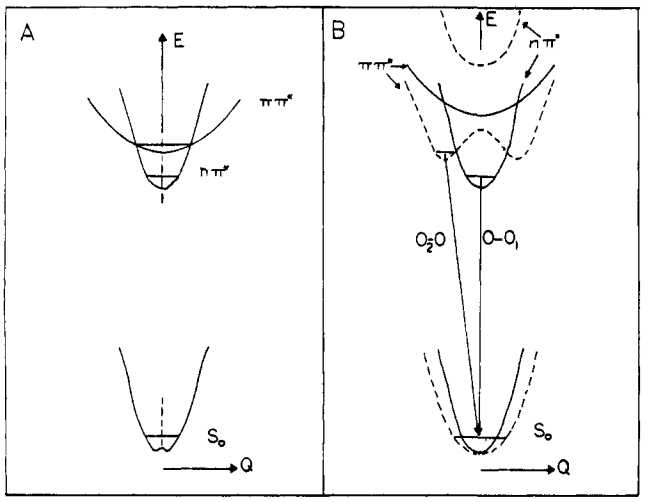

Figure 7. Schematic *p*-chlorobenzaldehyde triplet state potential curves for displacement along the CHO torsional coordinate illustrating various models characterizing the phosphorescence. Curves are drawn symmetric about a planar conformation. O_1-O, O_2-O refer to the two observed "origin" bands discussed in the text: (a) proposed curves for the free molecule in the vapor; (b) illustrating two sites — and - - - in crystalline methylcyclohexane. The two emissions are from the lowest triplet states in each site.

other state is $^3n\pi^*$-like and its energy minimum along the torsional coordinate is taken at the ground state geometry in agreement with the vibrational analysis of subspectrum I.

We now proceed to explain the observed deuterium isotope effects within the context of a two-site model. The average bond length in a free molecule generally decreases upon deuteration by 0.002–0.005 Å units, i.e., 0.25–0.3%.[23] This change is not expected to alter the way a deuterated derivative substitutes in the lattice. Thus both deuterated and undeuterated derivatives are expected to occupy identical sites in the matrix, each site showing its own deuterium isotope effects. The small difference in molecular size upon deuteration will lead to a difference in London dispersion forces acting on the molecules. This difference is expected to be minimum for the monodeuterio derivative and to increase in polydeuterated ones.

Tudron, Van Pruyssen, and Colson[24] have studied site effects on the triplet lifetimes of mono- and dideuteriobenzenes in low-temperature hosts. A small, but consistent, difference in the lifetime of the two orientationally dissimilar deuterated isomers was observed (1.5 ± 1.5% for C_6H_5D in C_6D_6 and 5.3 ± 1.5% for C_6H_5D in sym-$C_6H_3D_3$). The isomerization in benzene is believed to originate from the distortion of its lowest triplet state by vibrational electronic interactions.[25] This difference (in lifetimes) is suggested to arise from intermolecular contributions to the isotope effect on excited state lifetimes. These intermolecular effects supposedly act upon the radiative decay rate.[24]

Theoretical models which explain deuteration effects on radiative properties of simple molecules emphasize either (1) isotope effects on radiationless transition rates[26] by increasing density of the ground vibrational levels in the vicinity of the excited triplet state or by reducing the Franck-Condon factors governing intersystem crossing and thereby slowing radiationless transitions, or (2) isotope effects on vibronic matrix elements via changes in the nuclear motion[27,28] or vibrational frequency.[29-31] All these models are intramolecular in nature.

The deuterated benzenes study[24] represents a violation of these theoretical models, although the magnitude is minor. The difference in decay rates in the two sites was found to depend on the number of substituted deuterium atoms, i.e., it increases on going from benzene-d_1 to *p*-dideuteriobenzene. If such an effect is operative in the PCB/MCH systems, it is hard to understand why the effect of increasing the number of deuterium substitutions does not lead to a gradual change in radiative properties as found for benzene. This disappearance of subspectrum I in PCB-d_1 and its reappearance in PCB-d_4 is difficult to explain. This high sensitivity of PCB phosphorescence to the "presumed" site geometries necessitates the assumption of a very large intermolecular contribution to the isotope effects on radiative properties of the lowest triplet state(s). No such abnormally large intermolecular effect has been reported nor appears to be justified by existing theories of radiationless transitions.

The 4.2 K phosphorescence excitation spectrum of PCB in MCH is shown in Figure 6 for the $S_1(n\pi^*) \leftarrow S_0$ region. For the purpose of the discussion in this paper we focus on the origin band at 26 652 cm^{-1} and the bands 28 and 94 cm^{-1} to the blue. Because of the low frequency of these bands they cannot be assigned as vibronic transitions.[7] We suppose, for the moment, that these bands correspond to secondary sites, with the 26 652-cm^{-1} band as the primary site and generate corresponding site origins in the phosphorescence spectrum. In this case, the 94-cm^{-1} band corresponds to the O_2–O phosphorescence origin, the 28 cm^{-1} band to the O_1–O phosphorescence origin and the 26 652-cm^{-1} band to the O_2–104 phosphorescence band. Since the excitation spectrum reflects the intensity distribution in the phosphorescence spectrum, the intensity of site-generated origins should correspond in both phosphorescence and excitation spectra. They do not, however, the O_1–O phosphorescence line being the most intense of the three emission lines whereas its supposed site-generated counterpart in the excitation spectrum (the 28-cm^{-1} line) is distinctly the weakest.

The broadness of the 28- and 94-cm^{-1} bands suggests that phonon side-band assignment is a more plausible one for these bands. Further, upon laser excitation at 3000 Å, PCB-h_5 shows a very weak site emission at 213 cm^{-1} to the blue of the principal site and has an identical two-subspectra pattern. The identical spectra from the two sites is evidence that the subspectra themselves are not site generated.

We therefore conclude that although the multiple site model might provide a simple interpretation, neither the observed deuterium isotope effect nor the excitation spectrum support this model.

(6) Two Triplet States Arising from a Single Ground State Molecular Ensemble. The inadequacy of the two-site model forces us to consider a model based on the following assumptions:

(i) The sequence of the zero-order states in the free molecule, Figure 7A, is preserved but the spacing is decreased by the MCH crystal field.

(ii) The resultant states are expressed by wave functions

$$^3x_i = a_i \cdot {}^3n\pi^* + b_i \cdot {}^3\pi\pi^*$$

where a_i and b_i contain both vibrational-electronic and host-guest interactions. The electronic wave functions, $^3n\pi^*$ and $^3\pi\pi^*$, are considered to be adiabatic and the coupling mode is τ(CHO).

(iii) Subspectra I thus originates from a state with $^3n\pi^*$ parentage, x_1, i.e., $a_1 \gg b_1$, while subspectrum II originates from a second state, x_2, with $^3\pi\pi^*$ parentage, i.e., $b_2 \gg a_2$.

(iv) Radiationless relaxation between the two triplet states, produced via vibronic and crystal field interactions, is slow so that the main radiationless channel is through the lattice phonons.

A small internal conversion rate constant might be justified by large geometric dissimilarity between the two states, i.e., very small Franck-Condon factors and/or the small density of vibrational states in the vicinity of the two zero-point levels.[32]

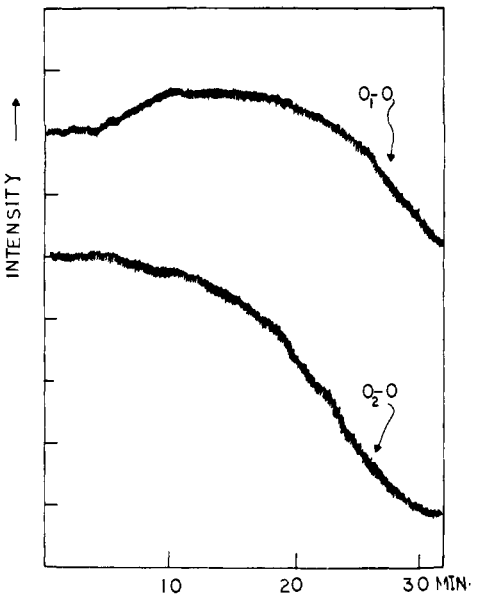

Figure 8. Variation of intensity (in arbitrary units) vs. warm-up time (after evaporation of liquid helium) of the two phosphorescence origins of *p*-chlorobenzaldehyde in methylcyclohexane. The final temperature is approximately 10 K.

Deuterium isotope effects on the spectra can be understood in terms of deuterium shifts of the zero points of the two states. The O-O band of the $^3n\pi^* \rightarrow S_0$ emission of benzaldehyde is known to blue shift by ca. 50 cm^{-1} on aldehyde group deuteration,[7] while the O-O bands of the $^3\pi\pi^* \rightarrow S_0$ emissions for both benzaldehyde[7] and PCB[14] are not sensitive to aldehyde group deuteration. The $n\pi^*$ shift is due to certain aldehyde group frequencies strongly decreasing in the excited state which do not occur in $\pi^* \leftarrow \pi$ excitation. Thus, this shift may be reasonably transferred to aldehyde group deuteration of PCB. The result is that the zero-order $^3\pi\pi^*$ zero-level energy will decrease to a near degeneracy with the $^3n\pi^*$ zero level and probably will lie just below it. Thus in PCB-d_1, the unique emission occurs from the strongly coupled lowest excited level, $a_1 \sim b_1$. Ring deuteration on the other hand will preserve the sequence of zero-order states and even increase the spacing giving rise to two emissions in PCB-h_5, -d_4, and -d_5.

Although this model explains the observed intramolecular deuteration effects, it runs into a serious difficulty. Subspectrum II corresponds to unrelaxed phosphorescence from an excited polyatomic molecule, with many vibrational modes embedded in a low-temperature environment. This interpretation represents a violation of Kasha's rule.[33]

Fluorescence from upper excited states and higher vibronic levels of the first excited states have been observed.[34] The process of internal conversion and fluorescence combine states of the same multiplicity and hence both processes may have approximately the same rates. For phosphorescence, however, spin forbiddeness requires the internal conversion to occur on a millisecond time scale for an upper state emission to be observed. Thus optical radiation from the upper state II necessitates a strong prohibition for radiationless relaxation from this state to the lowest electronic state I. Slow radiationless relaxation from the upper $^3\pi\pi^*$ of a closely spaced states system was suggested for the case of 5-methyl-1-indanone in *n*-hexane at temperatures higher than 20 K.[35] The upper state phosphorescence appears, and is enhanced, as the temperature of the sample rises, suggesting its classification as thermalized phosphorescence.[2]

In order to test this model the O_1-O and O_2-O band intensities in PCB-h_5 were monitored with increasing temperature. The results, Figure 8, show that although the O_2-O origin monotonically decreases in intensity as temperature increases, the O_1-O origin intensity increases before onset of decay. Thus the population of O_1 initially increases as that of O_2 decreases. This experiment clearly eliminates thermal population of O_2. The results are consistent in a qualitative way with coupling of the two states through lattice phonons, e.g., increasing density of lattice phonon states increases the internal conversion probability between state II and state I. Further increase in temperature is expected to increase the radiationless rate to the ground state.

Conclusions

The spectra of PCB/MCH isotopes have been used to demonstrate that the multiple phosphorescence of *p*-chlorobenzaldehyde in MCH observed at 4.2 K is not due to aggregates or different solvent phases. Although two sites have not been directly eliminated, phosphorescence excitation experiments and the large isotopic effects on the radiationless relaxations are not consistent with this possibility. It is thus argued that the two phosphorescences occur from two states generated from a single molecular ensemble. A model involving slow radiationless relaxation between two triplet states coupled by concerted host-guest and vibrational-electronic interactions is proposed. In the context of this model, isotope effects are largely due to changes in the coupling details through modulation of the energy gap between the zero-point levels in the zero-order potential surface.

The principal difficulty is that the efficiency of the host phonon decay channel is postulated to be small. In other words, PCB molecules, even in the MCH solid environment, are postulated to act nearly like relaxed free molecules, implying that the MCH-PCB interaction is small. This is to be contrasted to the normal relaxive behavior of PCB in MCH-d_{14} (unique phosphorescence with normal isotope effects), where the host-guest interaction, as measured by the larger gas crystal shift, is substantial.

The thermalization experiments are consistent with small coupling of the two emitting states through lattice phonons, but not unambiguously so. Further experiments similar to those in pyrazine[36] at lower temperatures than 4.2 K may elucidate the details of electron-phonon and spin-phonon radiationless channels. Both the suggested multisite and the two-state mechanisms suggest inadequacy of models of radiationless transitions to describe intermolecular contributions to relaxation processes between closely spaced states.

Acknowledgments. The authors acknowledge the close cooperation of Dr. Ronald Ruden in synthesizing the isotopic derivatives, a gift of PCB-d_1 from Professor D. S. Tinti of the University of California at Davis, assistance of Ms. S. Hankin, and discussion with Mr. Ilker Ozkan. Criticism of an earlier version of the manuscript by Professor M. A. El-Sayed, UCLA, Professor S. P. McGlynn, Louisiana State University, and Dr. M. Koyanagi, Kyushu University, Japan, has been very useful.

References and Notes

(1) (a) Supported by NSF Grant No. MPS-71-03359-A05; (b) M. Koyanagi and L. Goodman, *Chem. Phys. Lett.*, **21**, 1 (1973).
(2) H. Hayashi and S. Nagakura, *Mol. Phys.*, **27**, 696 (1974).
(3) S. W. Mao and N. Hirota, *Mol. Phys.*, **27**, 309 (1974); **27**, 327 (1974).
(4) A. M. Nishimura and D. S. Tinti, *Chem. Phys. Lett.*, **13**, 278 (1972).
(5) M. Souto, P. Wagner, and M. A. El-Sayed, *Chem. Phys.*, **6**, 193 (1974).
(6) A. J. Duben, L. Goodman, and M. Koyanagi, "Excited States", Vol. I., E. C. Lim, Ed., Academic Press, New York, N.Y., 1974, p 295.
(7) L. Goodman and M. Koyanagi, *Mol. Photochem.*, **4**, 369 (1972).
(8) P. J. Wagner, *Acc. Chem. Res.*, **4**, 168 (1974).
(9) PCB-d_1 was prepared by metallation of the 1,3-dithlane derivative by *n*-butyllithium followed by hydrolysis of the product by deuterium oxide and mercuric chloride–mercuric oxide mixture, cf. D. Seebach, B. W. Erickson, and G. Singh, *J. Org. Chem.*, **31**, 4303 (1966).
(10) PCB-d_4 was prepared from chlorobenzene-d_5 by standard procedures. Friedel–Crafts acylation with acetic anhydride in CS_2[11a] afforded the *p*-chloroacetophenone-d_4. The requisite aldehyde was obtained from this

substance by the following sequence of reactions: oxidation with Br_2/OH^- [11b] to the corresponding acid, reduction to the alcohol with $LiAlH_4$,[11c] and subsequent oxidation to the aldehyde with ceric ammonium nitrate.[11d]
(11) (a) R. Adams and L. R. Noller, "Organic Syntheses", Collect. Vol. I, Wiley, New York, N.Y., 1941, p 109; (b) R. Levine and J. R. Stephens, *J. Am. Chem.*, **72**, 1642 (1950); (c) R. F. Nystrom and W. G. Brown, *J. Am. Chem. Soc.*, **69**, 2548 (1947); (d) W. S. Trahanovsky and L. B. Young, *J. Chem. Soc.*, 5777 (1965).
(12) This sample has been prepared by Rosenmund reduction of *p*-chlorobenzoyl chloride by deuterium gas, cf. A. F. Thomson and H. H. Cromwell, *J. Am. Chem. Soc.*, **61**, 1374 (1939).
(13) O. S. Khalil and L. Goodman, *J. Phys. Chem.*, **80**, 2170 (1976).
(14) O. S. Khalil and L. Goodman, *J. Chem. Phys.*, **65**, 4061 (1976).
(15) S. W. Hankin, O. S. Khalil, and L. Goodman, preparation for publication.
(16) H. G. Silver and J. L. Woods, *Trans Faraday Soc.*, **60**, 5 (1964).
(17) M. Koyanagi, R. M. Zwarich, and L. Goodman, *J. Chem. Phys.*, **56**, 3044 (1972).
(18) N. Kanamaru, M. E. Long, and E. C. Lim, *Chem. Phys. Lett.*, **26**, 1 (1974).
(19) H. J. Pownall and J. R. Huber, *J. Am. Chem. Soc.*, **93**, 6429 (1971).
(20) H. J. Pownall, R. E. Connors, and J. R. Huber, *Chem. Phys. Lett.*, **22**, 403 (1973).
(21) H. J. Pownall and W. W. Mantulin, *Mol. Phys.*, **31**, 1393 (1976).
(22) S. Y. Chu and L. Goodman, *J. Mol. Spectrosc.*, submitted for publication.
(23) V. W. Laurie and D. R. Herschbach, *J. Chem. Phys.*, **37**, 1687 (1962).
(24) F. B. Tudron, J. M. Van Pruyssen, and S. D. Colson, *J. Chem. Phys.*, **63**, 2086 (1975).
(25) J. M. Van Pruyssen and S. D. Colson, *Chem. Phys.*, **6**, 382 (1974).
(26) J. W. Robinson and P. Frosch, *J. Chem. Phys.*, **37**, 1962 (1962); **38**, 1187 (1963).
(27) A. C. Albrecht, *J. Chem. Phys.*, **33**, 156 (1960).
(28) P. M. Johnson and L. Ziegler, *J. Chem. Phys.*, **56**, 2169 (1972).
(29) G. Orlandi and W. Siebrand, *Chem. Phys. Lett.*, **15**, 465 (1972).
(30) G. Orlandi and W. Siebrand, *J. Chem. Phys.*, **58**, 4513 (1973).
(31) S. F. Fischer and E. C. Lim, *Chem. Phys. Lett.*, **14**, 40 (1972).
(32) E. W. Schlag, S. Schneider, and S. F. Fischer, *Annu. Rev. Phys. Chem.*, **22**, 465 (1971).
(33) M. Kasha, *Discuss. Faraday Soc.*, **9**, 14 (1950).
(34) J. B. Birks, "Organic Molecular Photophysics", Vol. 2, Wiley, New York, N.Y., 1975, Chapter 9, and references therein.
(35) M. Long and E. Lim, *Chem. Phys. Lett.*, **20**, 413 (1973).
(36) L. Hall and M. A. El-Sayed, *Chem. Phys.*, **8**, 272 (1975).

Radiation Chemistry of Aqueous Cyanide Ion[1]

B. H. J. Bielski* and Augustine O. Allen

Contribution from the Department of Chemistry, Brookhaven National Laboratory, Upton, New York 11973. *Received January 28, 1977*

Abstract: Dilute KCN solutions, irradiated with γ rays in the presence of N_2O, give radicals $CONH_2$ which react quantitatively by disproportionation to yield equal amounts of cyanate and formamide. In the absence of N_2O, the radicals $CONH_2$ and H_2CN are formed and interact to yield a more complicated spectrum of products.

Exposure of aqueous solutions to high-energy radiations results in attack on solutes by hydrated electrons and radicals OH and H. The radiation chemistry of the solute consists of a resulting series of reactions. The radiation chemistry of cyanide solutions is of interest because of the relationship of cyanide to the halides, the radiation chemistry of which has been much studied, and because of its possible role in prebiological chemical evolution on the primitive earth. Photochemical or thermal treatment of cyanide solutions has been found to yield adenine and other interesting compounds.[2,3] Since far-ultraviolet light, penetrating the primitive oxygen-free atmosphere, could produce hydrated electrons and OH radicals in the surface layer of the oceans, study of the radiation chemistry of cyanide might also be relevant.

Recent pulse-radiolysis studies[4,5] have established the nature of the initially formed radicals in HCN and CN^- solutions. Some data on yields of the final products, especially from acid solutions, are reported by Ogura et al.[6,7] The present work reports detailed product analyses from irradiation of cyanide solutions at pH 11, with and without addition of N_2O to convert solvated electrons to OH radicals.

Experimental Section

Irradiations. Most of the work employed ^{60}Co γ rays; two sources were used, with intensities differing by a factor of 7. Pulse radiolysis was carried out as previously described.[8] All irradiations and analyses (except as noted) were made at room temperature (~22 °C).

Materials. Baker Analyzed Reagent KCN was recrystallized. Solutions were made in triple-distilled water saturated with N_2, Ar, or N_2O after boiling to expel CO_2 and O_2. $K^{14}CN$ from Schwarz Bio Research Inc. was treated with barium salt to remove carbonate, then purified by distillation from an acid solution to an alkaline one in a Conway diffusion apparatus.[9] Other labeled compounds (for testing product identifications and behavior) were obtained from ICN Tracerlab.

Analytical Methods. Hydrogen and nitrogen gases were determined by chromatography as described elsewhere.[10] Hydrogen peroxide was determined by adding ceric sulfate to the solution and determining the resulting oxygen by gas chromatography along with the nitrogen. Carbonate was determined by a modification of Carpenter's method.[11] The solution was acidified and warmed to 48 °C for 20 min, then the evolved gas passed into a Varian Aerograph gas chromatograph. Evolution of CO_2 was, however, not quantitative at low concentrations and the method had to be calibrated with known solutions.

Cyanide was determined as the Ni complex[12] or by the chloramine-T method;[13] good agreement was found between the two methods.

Ammonia was determined by the Orion ammonia electrode, Model 95-10.[14]

Formamide was determined as formate after base hydrolysis, using the quinaldinium iodide method.[15] The difference between the NH_3 content before and after hydrolysis provided a check on the result.

Cyanate was determined by the amounts of CO_2 and ammonia formed in acid hydrolysis of irradiated solutions. Its appearance in considerable yields was verified by paper chromatography, but this did not provide a quantitative determination, since some decomposition occurred in the acidic chromatographic solution.

Formaldehyde was determined by the acetylacetone method.[16]

Nonvolatile products were determined by descending paper chromatography of irradiated $K^{14}CN$ solution on Whatman no. 1 filter paper with 1-butanol–acetic acid–water (4:1:5) developer. As the solution migrates down the paper, components are held back in strips occurring at different fractions R_f of the total distance to the solvent front. Positions of the strips were found by placing the paper on an x-ray plate. R_f values for numerous compounds are tabulated[17] for this particular solvent. For further identification, the paper was cut into strips and tested with various reagents. After tentative identification, authentic samples of the compounds were run for comparison. The compounds found and their R_f values are listed in Table I. For quantitative determination, strips were cut out and completely eluted with water and the ^{14}C was counted in Aquasol (New England Nuclear) on a Beckman liquid scintillation system.